MHD simulation of the Bastille day event

Jon Linker, Tibor Torok, Cooper Downs, Roberto Lionello, Viacheslav Titov, Ronald M. Caplan, Zoran Mikić, and Pete Riley

Citation: AIP Conference Proceedings **1720**, 020002 (2016); doi: 10.1063/1.4943803
View online: http://dx.doi.org/10.1063/1.4943803
View Table of Contents: http://scitation.aip.org/content/aip/proceeding/aipcp/1720?ver=pdfcov
Published by the AIP Publishing

MHD Simulation of the Bastille Day Event

Jon Linker[1,a),b)], Tibor Torok[1], Cooper Downs[1], Roberto Lionello[1], Viacheslav Titov[1], Ronald M. Caplan[1], Zoran Mikić[1] and Pete Riley[1]

[1]*Predictive Science Inc., 9990 Mesa Rim Road, Suite 170, San Diego CA, USA 92121*

[a)]linkerj@predsci.com
[b)]URL: www.predsci.com

Abstract. We describe a time-dependent, thermodynamic, three-dimensional MHD simulation of the July 14, 2000 coronal mass ejection (CME) and flare. The simulation starts with a background corona developed using an MDI-derived magnetic map for the boundary condition. Flux ropes using the modified Titov-Demoulin (TDm) model are used to energize the pre-event active region, which is then destabilized by photospheric flows that cancel flux near the polarity inversion line. More than 10^{33} ergs are impulsively released in the simulated eruption, driving a CME at 1500 km/s, close to the observed speed of 1700km/s. The post-flare emission in the simulation is morphologically similar to the observed post-flare loops. The resulting flux rope that propagates to 1 AU is similar in character to the flux rope observed at 1 AU, but the simulated ICME center passes 15° north of Earth.

INTRODUCTION

Coronal Mass Ejections (CMEs) are spectacular manifestations of solar activity; these immense eruptions (often associated with solar flares) propel plasma and magnetic flux outward from the Sun. As the largest impulsive energy release events in the solar system, CMEs (and accompanying flares) are of inherent scientific interest. They are also associated with the most severe space weather effects at Earth. CMEs are the primary cause of major geomagnetic storms, and are also associated with solar energetic particles (SEP) events. Both types of events can represent a significant hazard for humans and technological infrastructure.

The most extreme eruptive events on the Sun are typically characterized by very fast (> 1000 km/s) CMEs and X-class solar flares. There are many open scientific questions about such events, such as how is the energy released so impulsively? From a space weather perspective, given an observation of such an event at the Sun, can we predict its arrival at Earth and subsequent geo-effectiveness?

The July 14, 2000 ("Bastille Day") CME/Flare was one of the largest flare/CME events of solar cycle 23. The X5.7 flare began at 10:03UT, followed by an intense radiation storm that resulted in one of the 16 GLE events of cycle 23. The fast moving CME traveled outward initially at about 1700 km/s. The interplanetary CME (ICME) driven shock wave reached the Advanced Composition Explorer (ACE) spacecraft in about 28 hours and the magnetic cloud a few hours later, triggering a large geomagnetic storm. As a disk-centered event, it is an advantageous example for studying an extreme eruptive event via numerical simulation.

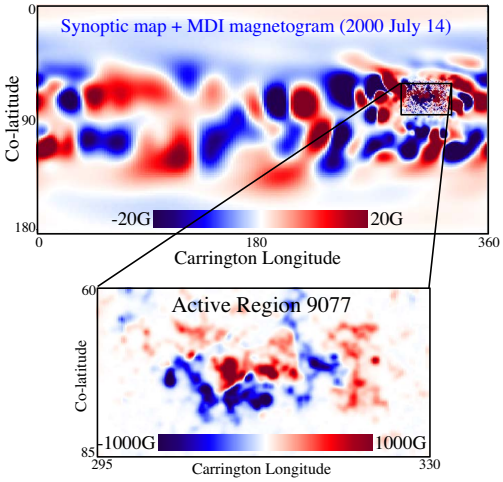

FIGURE 1. Magnetic map of B_r used for boundary conditions in the Bastille day simulation, derived from an MDI synoptic map and an MDI full-disk magnetogram (see text). The map was greatly smoothed to allow a coarse mesh to be used away from the active region (AR9077), while retaining as much structure as feasible within AR9077 (where the Bastille day eruptions originated). The maximum magnitude of B_r is 1986 Gauss.

Solar Wind 14
AIP Conf. Proc. 1720, 020002-1–020002-4; doi: 10.1063/1.4943803

In this paper, we describe a magnetohydrodynamic (MHD) simulation of the Bastille Day event. We use a thermodynamic MHD model [1], which allows us to simulate EUV and X-ray emission. We discuss the conditions necessary for storing adequate magnetic energy to power such extreme eruptions, we compare the simulated results with EUV and white-light emission, and we describe the properties of the simulated magnetic flux rope at 1 AU.

METHODOLOGY

A realistic simulation of a solar event starts from a description of the Sun's magnetic field. To specify the surface magnetic field for the Bastille day event, we combine a line-of-sight (LOS) Solar and Heliospheric Observatory (SOHO) Michelson Doppler Imager (MDI) synoptic map for Carrington rotation 1965 (7/10-8/6/2000) with a LOS MDI magnetogram measured at 7/14/2000 09:35UT to specify the radial magnetic field (B_r); see Figure 1. We first develop a thermodynamic MHD simulation of the global corona using the procedure, equations, and coronal heating specification described by [1]. In this model, the temperature at the lower boundary is 20,000 K, similar to the upper chromosphere, and the upper boundary is at 20 solar radii (R_S), beyond the sonic and Alfvén critical points. The solution is computed on a $401 \times 351 \times 471$ nonuniform spherical (r, θ, ϕ) mesh, with Δr in the range $4.5 \times 10^{-4} R_S$ (transition region) to $0.4 R_S$ (upper boundary), and latitudinal/longitudinal cells $\approx$ 0.0017-0.0019 radians in NOAA active region (AR) 9077, the source of the flare and CME. The coronal solution is relaxed for 160 Alfvén travel times (τ_A) or about 64 hours (1 $\tau_A \approx$ 24 minutes).

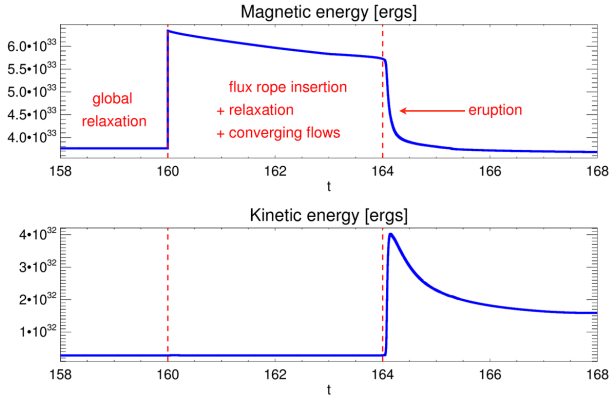

FIGURE 2. Magnetic (top) and kinetic (bottom) energy evolution in the simulation, focusing on the eruptive phase of the calculation. Time is in $\tau_A (\approx 24$ minutes). The global coronal solution is obtained by relaxing from $t = 0 - 160$. After insertion of the TDm configuration the system is relaxed further until $t = 162$, at which point flux cancellation is initiated by converging flows along the PIL. The system is destabilized shortly before $t = 164$.

To energize the AR, we introduce modified Titov-Démoulin (TDm) flux ropes [2] along the polarity inversion line (PIL) that separates the positive and negative B_r of the AR. The original Titov-Démoulin (TD) model [3] is an analytical model of a force-free coronal flux rope that has found wide application as an initial condition for idealized CME simulations [e.g., 4, 5, 6]. Out-of-equilibrium TD flux ropes have also been used in global coronal CME simulations [e.g., 7]. Starting from an equilibrium configuration is an important aspect of understanding the energy storage and release of CMEs. The TDm model [2] takes into account the pre-existing coronal magnetic field of the background solution as well as the potential field created by the flux rope current itself. With this technique, flux ropes can be introduced close to, but beneath, the threshold for eruption. In the simulations presented here, we further modified the TDm model to preserve the observed B_r distribution when inserting TDm ropes. This is a vital consideration because in the eruptive phase, the flux rope that propagates outward (eventually to 1 AU) is a combination of the inserted flux rope and the surrounding AR fields.

In practice, we first separately develop our pre-event flux-rope configuration with the same surface B_r distribution (B_{r0}) as the full coronal model. We choose the TDm flux-rope parameters such that the rope is stable with respect to the kink and torus instabilities [5, 8]. To preserve B_{r0}, we calculate the desired TDm flux rope and compute the photospheric B_r associated with this solution. We then subtract the new B_r distribution from the original B_{r0} and obtain a new potential field. We finally insert the TDm flux rope into this field, which re-introduces the subtracted B_r so that B_{r0} is preserved. This configuration is then relaxed to a force-free state using a zero-beta MHD model [solution of the momentum equation and Faraday's law with plasma pressure = 0, e.g., 9]. To insert the relaxed configuration into the global coronal model, we specify the vector potential $\mathbf{A}$. We subtract $\mathbf{A_{pot}}$ of the potential field solution from $\mathbf{A_{ZB}}$ of the zero-beta MHD solution, and then add $\mathbf{A_{ZB}} - \mathbf{A_{pot}}$ to the global coronal simulation ($\mathbf{A_{cor}}$). The simulation shown here used a chain of seven overlapping TDm flux ropes, which together form a single rope, to account for the highly elongated and curved PIL in the source region of the eruption (Figure 3 (d)). The configuration approached an approximately force-free equilibrium in $\sim 0.2 \tau_A$ during the zero-beta relaxation.

After triggering the CME (see next section), we follow its evolution to 1 AU using coupled coronal-heliospheric models [10]. The heliospheric calculation used a 486×264×583 nonuniform spherical mesh extending from 19-230R_S.

RESULTS

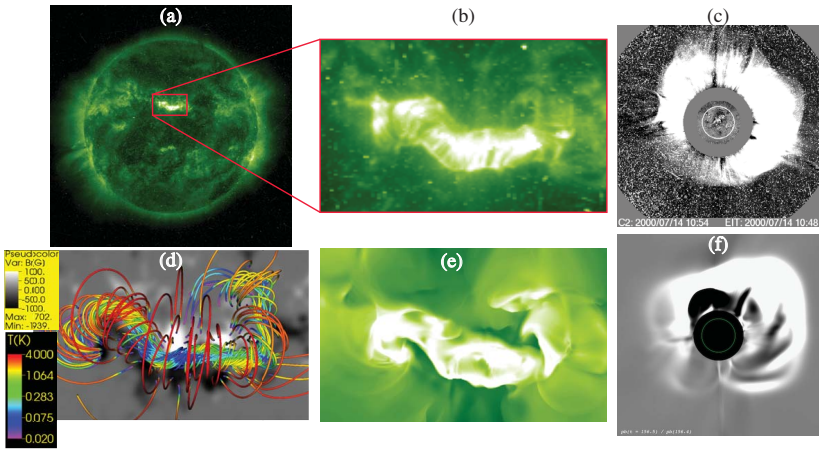

FIGURE 3. Comparison of observations from the Bastille Day Event (July 14, 2000) with an MHD simulation using TDm flux ropes to initiate a CME. (a) SOHO EIT 195Å observations of the X-class flare. (b) Closeup of EIT 195Å showing post flare loops in eruption. (c) Halo CME from SOHO LASCO C2 differenced white light images. (d) The resulting equilibrium flux rope after a chain of seven pre-relaxed TDm flux ropes is introduced into the thermodynamic MHD simulation. The field lines are colored by log(T) in 10^6 K; cold (prominence-like) plasma condenses on the flux rope. The gray scale image shows B_r at the boundary in Gauss. (e) Post-flare loops in 195Å from the simulated eruption. (f) White-light halo (from running ratio of polarization brightness) from the simulated CME.

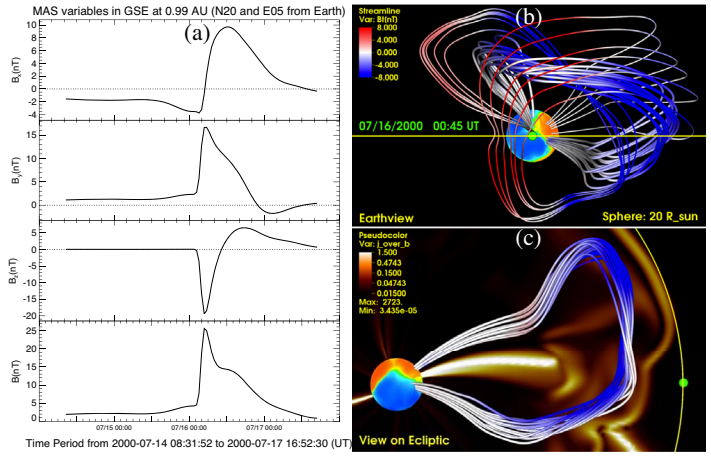

FIGURE 4. (a) Magnetic field signature of the simulated ICME at 1 AU. (b) Selected magnetic lines in the ICME as viewed from Earth. (c) Magnetic field lines in the ICME as viewed from above the ecliptic plane. The colored sphere is at the position of the inner boundary of the heliospheric calculation. The small green sphere shows the approximate Earth position.

Figure 2 shows the evolution of the magnetic and kinetic energies in the coronal domain before and after eruption. After we introduce the configuration of seven merged flux ropes into the coronal calculation ($t = 160$), the solution is close to being force-balanced but is not in thermal equilibrium. Flows and cold plasma condensations appear along the flux rope field lines, possibly arising from thermal non-equilibrium [11]. The system is relaxed to $t = 162$, during which time the numerical dissipation (enhanced by the thermal flows) leads to some energy loss. Converging flows that cancel flux are then introduced along the PIL [12] until $t = 164$, at which point the configuration destabilizes. The full eruption commences shortly thereafter, releasing 1.3×10^{33} ergs in about 4 minutes ($0.16\tau_A$); about 31% (4×10^{32} ergs) is converted into kinetic energy. The simulated CME reached a speed of about 1500km/s.

It is interesting to compare the energies stored and released in the simulated AR to the AR potential field and open field energies W_{pot} and W_{open}, respectively. (For a given magnetic flux distribution, the open field is the magnetic field with all field lines beginning at the photosphere and extending to infinity.) Previously, it has been argued [13, 14] that the energy of a force-free field cannot exceed W_{open}; if this is correct, it places an upper limit on the amount of free energy that can be stored, $W_{open} - W_{pot}$. We refer to this as the Maximum Free Energy or MFE. We computed $W_{pot} = 1.71 \times 10^{33}$ ergs and $W_{open} = 5.76 \times 10^{33}$ ergs for AR9077, so MFE = 4.05×10^{33} ergs. The total energy stored in the simulated AR9077 when the flux rope configuration is introduced is 2.6×10^{33}ergs, or 64% of the MFE. Some of this energy was reduced during the relaxation and flux cancellation phases (flux cancellation also reduces W_{open}), but 32% of the original MFE is released impulsively. Our results suggest that the MFE may be a good guide to the maximum energy release of very large events.

Figure 3 compares the simulated eruption with observations. In Figure 3(a) we see emission from the flare in the SOHO Extreme Ultraviolet Imaging Telescope (EIT) 195Å filter at 11:12UT, ~41 minutes after the maximum flare phase seen in GOES at 10:24UT. Figure 3(b) shows a closeup of emission in the post-eruptive loops; these were noted for their striking morphology and pattern of growth from west to east, as was also seen in Transition Region and Coronal Explorer (TRACE) images. The large halo CME observed with the SOHO Large Angle and Spectrometric Coronagraph (LASCO) is shown in Figure 3(c). Figure 3(d) shows magnetic field lines colored by temperature in the TDm flux rope after it has been introduced into the coronal simulation and relaxed. Cold, dense, prominence-like plasma appears along the field lines, accompanied by flows. Figure 3(e) shows simulated EIT 195Å emission from the computation, which reproduces the morphology of the post-eruptive loops. The west-to-east growth (not shown) is also reproduced. Figure 3(f) displays a simulated white-light image (running ratio of polarization brightness). A halo-like structure forms from the simulated CME.

The Bastille Day ICME triggered a large geomagnetic storm at Earth. The ICME decelerated during its propagation, arriving at 1 AU with a speed of ~1150 km/s and a maximum $|\mathbf{B}|$ of ~50nT at about 19UT on 7/15/2000 [15, 16]. Figure 4 shows results from the heliospheric simulation of the ICME. Our simulated ICME arrived about seven hours later at 2UT on 7/16, with a speed of ~900 km/s and a maximum $|\mathbf{B}|$ of ~27nT, about 15° northward of Earth (Figure 4(a)). A weaker signature was seen at Earth's location. Figure 4(b) shows a view from Earth of the flux rope, colored by the magnitude of B_θ; positive B_θ is predominantly in the direction of negative B_Z at Earth. We see that $+B_\theta$ ($-B_Z$) arises from the azimuthal fields wrapping the core of the flux rope. The structure of the simulated ICME is qualitatively consistent with the flux rope inferred from observations [16]: a full rotation of $-B_Z$ from positive to negative, and $B_X, B_Y > 0$ occurring as the spacecraft passes through a left-handed flux rope below its axis. Figure 4(c) shows field lines in the core of the flux rope viewed looking down on the ecliptic plane. The core of the flux rope connects back to the Sun (the colored sphere is actually the inner boundary of the heliospheric calculation at $19R_S$).

SUMMARY

We have presented results from a simulation of an extreme event: the July 14, 2000 flare/CME. The simulation reproduces the rapid, strong energy release, and emission and white-light morphology of the event. The structure of the simulated ICME is similar to the flux rope inferred from ACE measurements, but it is weaker and northward of the real event. The propagation direction of the simulated CME is set very low in the corona, and did not change significantly in several numerical experiments. A possible reason for the discrepancy with observations is that the smoothing of the background magnetic field may have affected the initial CME trajectory. We plan to investigate this in future studies.

ACKNOWLEDGMENTS

Work at Predictive Science was supported by AFOSR, the NASA programs LWS C-SWEPA project, LWS team on Flux Ropes, LWS team on interplanetary B_Z, and HSR, and by the NSF programs FESD, SHINE and Solar Terrestrial. Computational resources were provided by the NSF supported Texas Advanced Computing Center (TACC) in Austin and the NASA Advanced Supercomputing Division (NAS) at Ames Research Center.

REFERENCES

[1] R. Lionello, J. A. Linker, and Z. Mikić, ApJ **690**, 902–912 (2009).
[2] V. S. Titov, T. Török, Z. Mikić, and J. A. Linker, ApJ **790**, 163 (2014).
[3] V. S. Titov, and P. Démoulin, A&A **351**, 707–720 (1999).
[4] I. I. Roussev, T. G. Forbes, T. I. Gombosi, I. V. Sokolov, D. L. DeZeeuw, and J. Birn, ApJ **588**, L45–L48 (2003).
[5] T. Török, and B. Kliem, ApJ **630**, L97–L100 (2005).
[6] C. J. Schrijver, C. Elmore, B. Kliem, T. Török, and A. M. Title, *Ap. J.* **674**, 586–595 (2008).
[7] N. Lugaz, C. Downs, K. Shibata, I. I. Roussev, A. Asai, and T. I. Gombosi, ApJ **738**, 127 (2011).
[8] B. Kliem, and T. Török, Phys. Rev. Lett. **96**, 255002 (2006).
[9] Z. Mikić, and J. A. Linker, ApJ **430**, 898–912 (1994).
[10] R. Lionello, C. Downs, J. A. Linker, T. Török, P. Riley, and Z. Mikić, ApJ **777**, 76 (2013).
[11] Z. Mikić, R. Lionello, Y. Mok, J. A. Linker, and A. R. Winebarger, ApJ **773**, 94 (2013).
[12] J. A. Linker, Z. Mikić, R. Lionello, P. Riley, T. Amari, and D. Odstrcil, *Phys. of Plasmas* **10**, 1971–1978 (2003).
[13] J. J. Aly, ApJ **375**, L61–L64 (1991).
[14] P. A. Sturrock, ApJ **380**, 655–659 (1991).
[15] C. W. Smith et al., Sol. Phys. **204**, 227–252 (2001).
[16] V. B. Yurchyshyn, H. Wang, P. R. Goode, and Y. Deng, ApJ **563**, 381–388 (2001).